frontiers in Materials

TYPE Original Research
PUBLISHED 04 March 2026
DOI 10.3389/fmats.2026.1753934

OPEN ACCESS

EDITED BY
Jobin Varghese,
Fraunhofer Institute for Ceramic Technologies and Systems (FHG), Germany

REVIEWED BY
Ahmad KASSAS,
Lebanese International University, Lebanon
Xiongli Liu,
Inner Mongolia University, China

*CORRESPONDENCE
Xilin Wang,
wang.xilin@sz.tsinghua.edu.cn

RECEIVED 25 November 2025
REVISED 03 February 2026
ACCEPTED 20 February 2026
PUBLISHED 04 March 2026

CITATION
Bian Y, Feng Y, Liu Y, Yin G, Liu F, Liu Z, Song J, Zhang P and Wang X (2026) Room-temperature rapid fabrication of porous ZnO ceramics by flash sintering with carbon electrodes.
Front. Mater. 13:1753934.
doi: 10.3389/fmats.2026.1753934

Room-temperature rapid fabrication of porous ZnO ceramics by flash sintering with carbon electrodes

Yalin Bian[1], Ying Feng[1], Yifei Liu[2], Guilai Yin[3], Fangji Liu[3], Zhuo Liu[2], Jiming Song[1], Pengfei Zhang[1] and Xilin Wang[2]*

[1]China Electric Power Research Institute, Beijing, China, [2]Engineering Laboratory of Power Equipment Reliability in Complicated Coastal Environments, Tsinghua Shenzhen International Graduate School, Tsinghua University, Shenzhen, China, [3]Electric Power Science Research Institute, State Grid Jiangxi Electric Power Co. Ltd., Nanchang, China

Porous ZnO ceramics with tunable pore structures were prepared in air at room-temperature via flash sintering using the pore-former method in conjunction with a flash sintering device based on a carbon electrode structure. By employing various amounts of basic zinc carbonate as the pore-former, ceramics with adjustable porosity were obtained. The results showed that as the content of basic zinc carbonate increased, both the sample porosity and average pore size increased significantly; at high contents, millimeter-scale macropores and well-developed mesoporous structures were achieved. Flash sintering enabled rapid densification within a very short time, demonstrating high efficiency and energy-saving advantages. Mechanical property tests indicated that increased porosity led to decreases in Vickers hardness and fracture toughness. This study applies the room-temperature flash sintering technology to porous ceramic materials, expanding the application scope of the room-temperature flash sintering technology and providing a more efficient and energy-saving new method for the preparation of porous ceramic materials.

KEYWORDS
carbon electrodes, mechanical properties, pore-forming agent method, porous ZnO ceramics, rapid sintering, room-temperature flash sintering

1 Introduction

Porous ceramics refer to ceramic materials with a large number of pore structures. They have been applied in various industrial fields, such as catalysis, heat insulation, sound insulation, biomedicine, etc. Porous ZnO ceramics are commonly used in various sensors and photocatalytic devices (Shahini et al., 2018; He et al., 2024; Lin et al., 2025; Carlesso et al., 2013; Shakir and Géber, 2023).

Current research on porous ceramics mainly focuses on methods for introducing pores into the preform. Scholars have discovered various effective methods, such as the pore-forming agent method, foaming method, freeze-drying method, 3D printing method, and sol-gel method, etc. (Chen et al., 2023).

During the subsequent sintering process, traditional sintering techniques are still employed. Traditional sintering requires long periods of high-temperature heating to achieve densification. Energy consumption is extremely high and emission issues are concerns. Pressureless sintering and hot pressing methods typically require

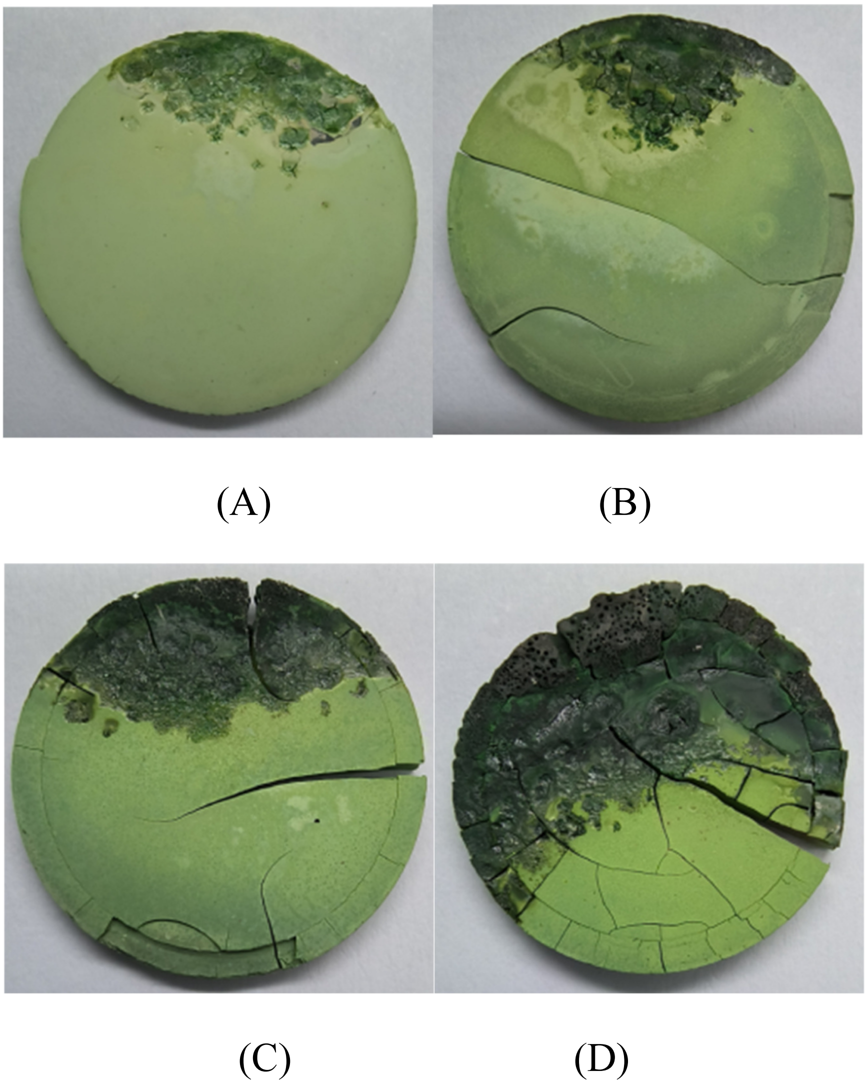

FIGURE 1
The surface morphology photographs of ZnO ceramics flash-sintered with different pore-former contents: **(A)** PF30; **(B)** PF50; **(C)** PF70; **(D)** PF90.

the preform to remain in a high-temperature environment above 1,000 °C for a long time. This limits the large-scale production of porous ceramics. There is an urgent need to develop a new technology. It must ensure the pore structure and mechanical strength of porous ceramics while enabling rapid sintering at low temperature.

Flash sintering is a novel electric field-assisted sintering technology that can significantly reduce the required sintering temperature and duration by applying an electric field to the green body. During flash sintering, the electrical resistivity of the body drops as the temperature rises, triggering runaway Joule heating and causing rapid densification in a short period (Cologna et al., 2011; Naik et al., 2016). Traditional flash sintering reduces the required temperature but still relies on a high-temperature furnace. Recently, researchers have optimized the sintering environment and equipment. They have also regulated the composition and properties of green bodies. This has enabled room-temperature flash sintering for various ceramics (Nie et al., 2018; Liu et al., 2020; Li et al., 2023; Zhao et al., 2024).

Most current research on flash sintering focuses on dense ceramics. Its application in porous ceramics remains largely unexplored. Developing a simple, rapid, and energy-efficient flash sintering technique for the fabrication of porous ceramics is of great significance.

In this study, a flash sintering device based on a carbon electrode structure was used together with the pore-former method to achieve room-temperature flash sintering of porous ZnO ceramics in air.

Compared with traditional sintering, this method significantly reduces both sintering time and energy consumption. Compared with Spark Plasma Sintering (SPS), our flash sintering method needs no extra pressure. The equipment is simpler and it starts at room temperature. It can also shorten sintering time and save energy. It is more suitable for the sintering of porous ceramics.

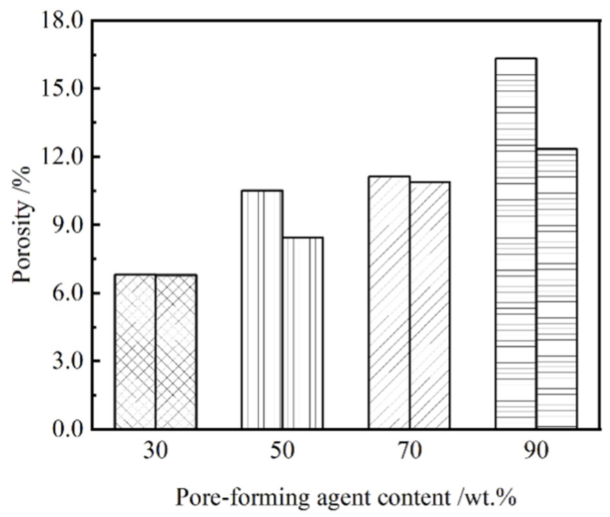

FIGURE 2
The porosities of ZnO ceramics flash-sintered with different pore-former contents.

2 Materials and methods

The starting powders were nano ZnO powder (10–20 nm, Suzhou Youzirconium NanoMaterials Company) and basic zinc carbonate powder (Tianjin Huasheng Chemical Reagent Company). The two powders were blended via ball milling to prepare four batches with basic zinc carbonate contents of 30 wt.%, 50 wt.%, 70 wt.%, and 90 wt.%, denoted as PF30, PF50, PF70, and PF90, respectively. Each powder blend was mixed with a 5 wt.% polyvinyl alcohol aqueous solution at a mass ratio of 10:1. A fixed amount of the slurry was then uniaxially pressed at 400 MPa into disk-shaped green bodies with a diameter of 20.0 mm and a thickness of approximately 2.00 mm. The green disks were heated at 400 °C for 2 h to remove the pore-former and allow the complete thermal decomposition of basic zinc carbonate, releasing CO_2 and water vapor, thereby generating the pore structure.

The flash sintering device employed a composite laminar carbon electrode structure previously developed for dense ceramics, in which graphite felt serves as a flexible extended electrode to effectively limit heat loss, generate thermal plasma, and ensure good electrical contact between the sample and the electrode. This structure minimizes current inhomogeneity and facilitates flash sintering at ambient starting temperature. Localized plasma-induced heating may occur during the process (Liu et al., 2025). Although the initial sintering environment was set at room temperature, localized high temperatures occurred during the actual sintering process. It initiated flash sintering.

In air, the green disk was mounted on the device and a voltage of 100 V was applied, immediately causing intense flashing of the sample. A constant current of 5 A was maintained for 90 s using a current source, after which power was shut off to complete the flash sintering process.

The relative density and open porosity of the samples were measured with the Archimedes method. This method quickly evaluates open pore structures in porous ceramics. Nitrogen adsorption (BET) and scanning electron microscopy (SEM) were also used. These provide multi-scale pore analysis. Microstructure was examined by SEM (HITACHI SU8010). Vickers hardness (XHVT-30Z) tests and fracture toughness measurements were conducted on representative samples for each composition. The data show consistent trends from the flash sintering process under controlled conditions. Pore structure parameters were evaluated using a specific surface area analyzer (BET, ASAP 2020M+C). X-ray diffraction (XRD, Bruker D8 Advance) was conducted to confirm phase purity and crystallinity.

Mechanical and porosity data are reported as mean values from three independent experiments. Error bars are not shown because measurements were performed under consistent conditions, and the observed trends were clear and reproducible. The reported values are representative of the material behavior under the specified flash sintering conditions.

3 Results and discussion

3.1 Porosity and morphology structure

Surface morphology photographs of porous ZnO ceramics flash-sintered with different pore-former contents are shown in Figure 1. As seen, higher contents of basic zinc carbonate result in a larger area of porous regions visible on the surface. When the basic zinc carbonate content reaches 90 wt.%, pores millimeter in size are visible to the naked eye.

The porosities of porous ZnO ceramics prepared with different pore-former contents are shown in Figure 2. As illustrated, with increasing basic zinc carbonate content, both the number and size of pores rise, leading to increased sample porosity. The highest porosity was observed in the PF90 group, as high as 16.3%. However, even when the content reached 90 wt.%, the measured porosity remained below 20%. This is because the Archimedes drainage method accounts only for open porosity, while closed pores are neglected, meaning the calculated porosity actually reflects the apparent pore volume. From the standpoint of molecular weights and the decomposition reaction equation, over 70% of the mass of basic zinc carbonate decomposes to ZnO, which remains in the green body. Thus, even if pure basic zinc carbonate is used to form the green body and flash sinter it, taking into account volume shrinkage, the final sample porosity would still be below 30%.

Figure 3 presents the SEM images of the microstructures of ZnO ceramics flash-sintered with varying pore-former contents. It can be seen that higher basic zinc carbonate content leads to more plentiful micro-pores post-sintering, with particularly apparent pore structures in the PF90 group. However, pore distribution becomes less uniform at higher pore-former contents, resulting in heterogeneous pore sizes and irregular macro-pores in PF90 samples, as clearly visible in SEM images.

3.2 Pore parameters

Figure 4 shows the nitrogen adsorption-desorption isotherms of porous ZnO ceramics flash-sintered with different pore-former contents. The curves are typical of type-IV isotherms with prominent hysteresis loops. Increased pore-former content results

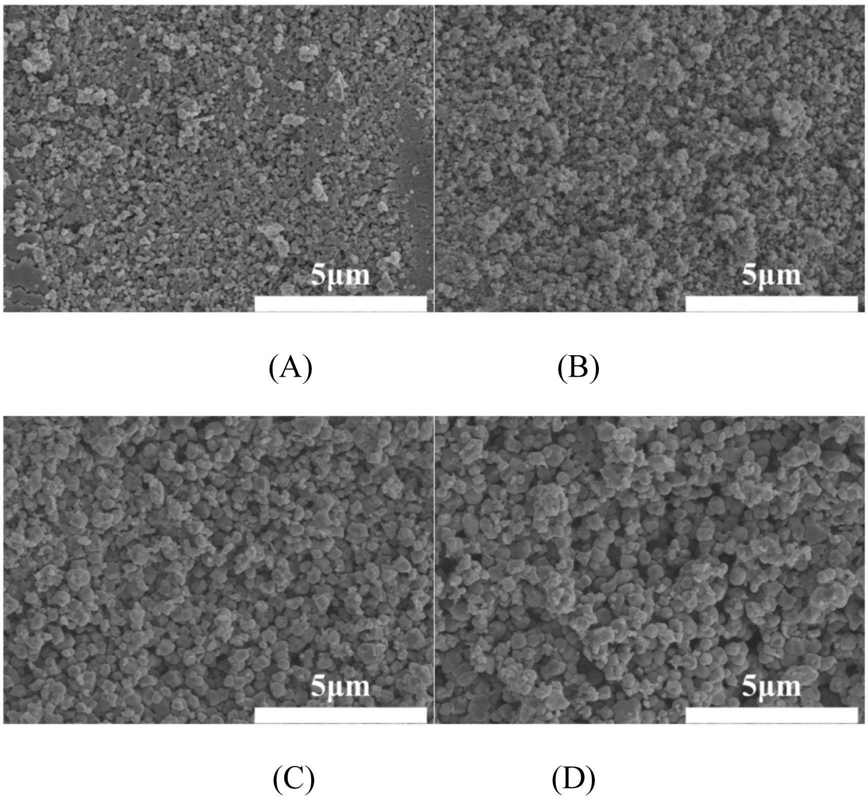

FIGURE 3
The SEM images of the microstructures of ZnO ceramics flash-sintered with different pore-former contents: **(A)** PF30; **(B)** PF50; **(C)** PF70; **(D)** PF90.

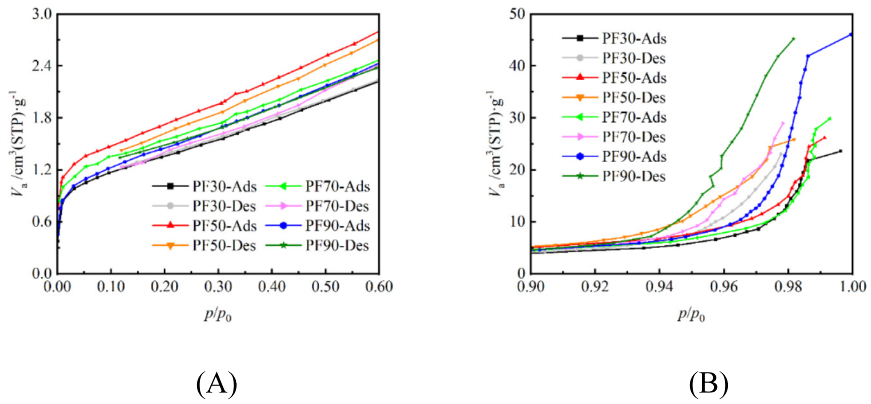

FIGURE 4
The nitrogen adsorption-desorption isotherms of ZnO ceramics flash-sintered with different pore-former contents: **(A)** The initial part of the curve; **(B)** The latter part of the curve.

in higher levels of nitrogen adsorption at high relative pressures, indicating that the total mesopore volume increases.

The pore size distributions of the samples are shown in Figure 5. The samples exhibit micro-, meso-, and macropore distributions; higher basic zinc carbonate content, especially in PF90, leads to a noticeable increase in large-sized pores, while PF30–PF70 show relatively similar pore size profiles.

For PF30–PF70 samples, the pore size distributions show similar profiles with a predominant mesopore population (2–50 nm), indicating a relatively uniform pore network at moderate pore-former contents. PF90 shows a bimodal distribution. The number of macropores increases significantly. These macropores are larger than 100 nm. This confirms a transition to a coarser pore structure. The pore structure is also interconnected.

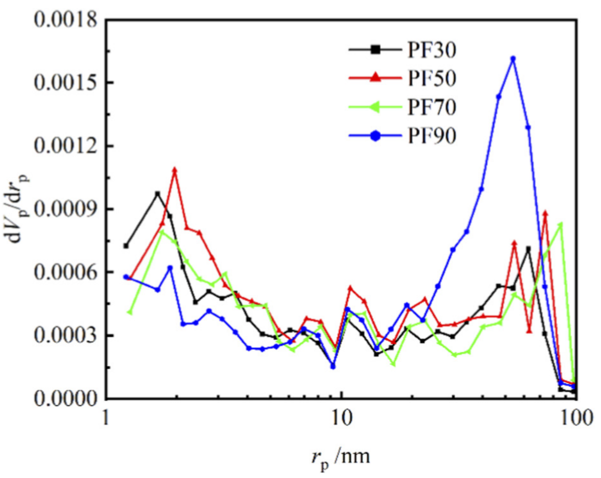

FIGURE 5
The pore size distributions of ZnO ceramics flash-sintered with different pore-former contents.

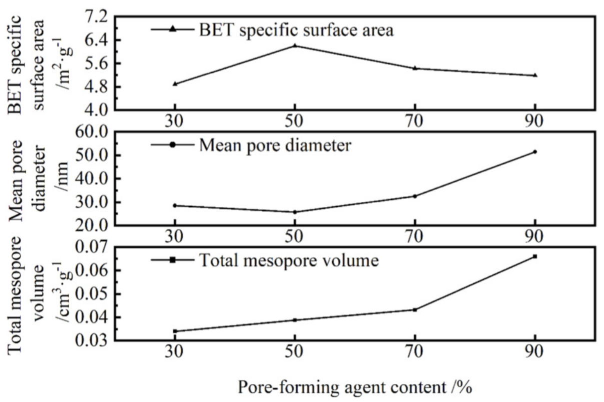

FIGURE 6
The pore parameters of ZnO ceramics flash-sintered with different pore-former contents.

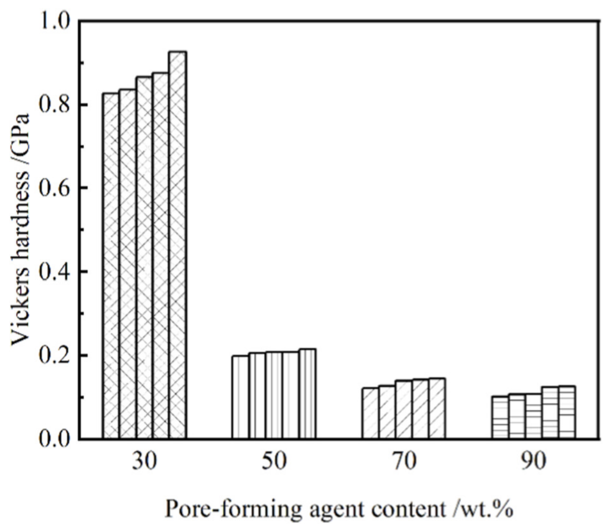

FIGURE 7
The Vickers hardness of ZnO ceramics flash-sintered with different pore-former contents.

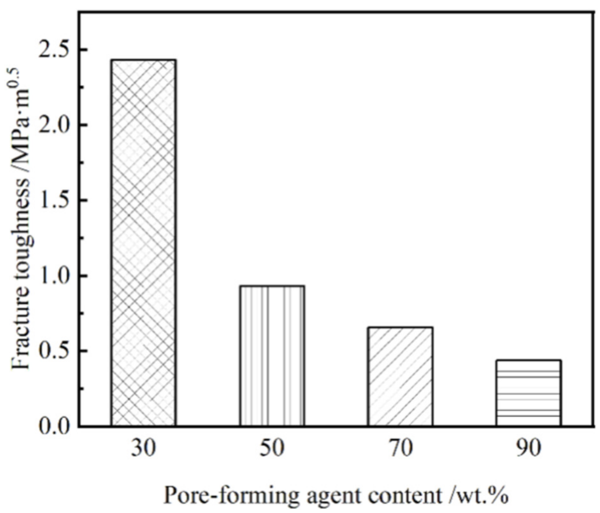

FIGURE 8
The fracture toughness of ZnO ceramics flash-sintered with different pore-former contents.

Pore parameters for flash-sintered porous ZnO ceramics with different pore-former contents—BET specific surface area, average pore size, and total mesopore volume—are presented in Figure 6. The data indicate that increasing content of basic zinc carbonate leads to larger total mesopore volumes and greater average pore sizes after flash sintering. This is because more pore-former generates more pores *in situ* upon thermal decomposition. At higher content, direct contact between basic zinc carbonate particles in the green body results in interconnected pores after removal, thus increasing average pore size.

BET specific surface area depends both on the number of pores and their sizes. At lower pore-former contents, as content increases, more pores form and pore wall surface area rises, giving higher BET surface areas. However, with further increases in pore-former, although the number of pores may continue to rise, the increasing pore size causes the total inner surface area per unit volume to decrease, so BET specific surface area gradually decreases. Accordingly, BET specific surface area increases and then decreases with increasing pore-former, attributable to a transition from fine, dispersed to coarser, interconnected pore structures and the trade-off between overall surface area and number of pores.

3.3 Mechanical properties

Figures 7, 8 show the Vickers hardness and fracture toughness of porous ZnO ceramics flash-sintered with different pore-former contents, respectively. As basic zinc carbonate content increases, both Vickers hardness and fracture toughness clearly decrease. When the content is 30 wt.%, the flash-sintered sample reaches

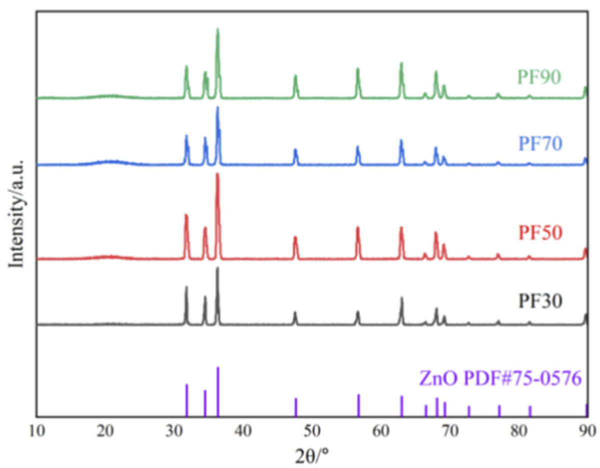

FIGURE 9
X-ray diffraction patterns of flash-sintered porous ZnO ceramics with different pore-former contents.

a Vickers hardness of 0.9261 GPa and a fracture toughness of 2.4320 MPa·m$^{0.5}$. Higher basic zinc carbonate content results in higher porosity, reducing the effective load-bearing area, with internal stress tending to concentrate at pores and thus lowering the ceramic hardness. More pores also provide additional sites and paths for crack propagation, facilitating crack extension between pores. Furthermore, the presence of pores reduces the interaction between bridging microstructures (such as grains) and cracks, diminishing the bridging effect. Therefore, at higher porosities, pores act as the main propagation path for cracks, lowering the fracture toughness of the ceramic.

Compared with conventionally sintered porous ZnO ceramics reported in the literature, flash-sintered samples exhibited comparable mechanical properties at similar porosity levels, while the processing time was reduced from hours to seconds, offering dramatic energy savings (Roy, 2015). This advantage is similar to the characteristics of other emerging low-temperature technologies (Wang et al., 2025). But flash sintering technology can achieve the same effect without the need for specialized pressure equipment or additional subsequent processing steps.

As the porosity increases, mechanical properties will decrease accordingly, which is consistent with the microscopic structure observation results shown in Figure 3. It can be seen from the figure that stress concentrates near the pores, promoting the expansion of cracks. The interconnected pore networks in high-porosity samples also prove this point.

3.4 Crystal structure analysis

Figure 9 shows the X-ray diffraction patterns of flash-baked porous ZnO ceramics with different contents of pore-forming agents. All samples show characteristic peaks corresponding to the hexagonal wurzite crystal structure of ZnO (JCPDS number 36-1451), indicating that the flash sintering process did not introduce any secondary phases or impurities. The sharp diffraction peaks indicate high crystallinity even under rapid sintering conditions. No peaks corresponding to basic carbonate zinc were detected, which confirmed that it had completely decomposed during the degreasing process.

4 Conclusion

Porous ZnO ceramics with different porosities were successfully prepared in air by combining the pore-former method with room-temperature flash sintering technology based on carbon electrodes. The basic zinc carbonate serving as the pore-former decomposes thermally during debinding, generating gas pores and leaving only ZnO as the final component. The experimental results indicate:

The porosity, pore size, and total mesopore volume of the ceramic samples increased significantly with increasing basic zinc carbonate content, reaching a porosity of up to 16.3% at 90 wt.% basic zinc carbonate.

When the basic zinc carbonate content was 30 wt.%, the Vickers hardness of the flash-sintered sample reached 0.9261 GPa and the fracture toughness 2.4320 MPa·m$^{0.5}$. Increasing porosity led to decreased ceramic hardness and fracture toughness. This work demonstrates highly efficient, low-energy-consumption sintering of porous ZnO ceramics and provides new strategies for the fabrication and application of porous ceramics. This work demonstrates highly efficient, low-energy-consumption sintering of porous ZnO ceramics and provides new strategies for the fabrication and application of porous ceramics.

Data availability statement

The original contributions presented in the study are included in the article/supplementary material, further inquiries can be directed to the corresponding author.

Author contributions

YB: Validation, Writing – review and editing, Writing – original draft, Resources, Investigation, Data curation. YF: Investigation, Writing – review and editing, Writing – original draft, Resources, Data curation, Validation. YL: Investigation, Data curation, Validation, Resources, Writing – review and editing, Writing – original draft. GY: Conceptualization, Methodology, Investigation, Writing – original draft. FL: Methodology, Conceptualization, Investigation, Writing – original draft. ZL: Methodology, Writing – original draft, Investigation, Conceptualization. JS: Writing – review and editing, Conceptualization, Investigation, Supervision. PZ: Investigation, Supervision, Writing – review and editing, Conceptualization. XW: Investigation, Project administration, Writing – review and editing, Funding acquisition.

Funding

The author(s) declared that financial support was received for this work and/or its publication. This work was supported by the

State Grid Corporation of China Science and Technology Project (No. 52180025000Z-289-LZ).

Conflict of interest

Authors GY and FL were employed by Electric Power Science Research Institute, State Grid Jiangxi Electric Power Co. Ltd.

The remaining author(s) declared that this work was conducted in the absence of any commercial or financial relationships that could be construed as a potential conflict of interest.

Generative AI statement

The author(s) declared that generative AI was not used in the creation of this manuscript.

Any alternative text (alt text) provided alongside figures in this article has been generated by Frontiers with the support of artificial intelligence and reasonable efforts have been made to ensure accuracy, including review by the authors wherever possible. If you identify any issues, please contact us.

Publisher's note

All claims expressed in this article are solely those of the authors and do not necessarily represent those of their affiliated organizations, or those of the publisher, the editors and the reviewers. Any product that may be evaluated in this article, or claim that may be made by its manufacturer, is not guaranteed or endorsed by the publisher.

References

Carlesso, M., Giacomelli, R., Günther, S., Koch, D., Kroll, S., Odenbach, S., et al. (2013). Near-net-shaped porous ceramics for potential sound absorption applications at high temperatures. *J. Am. Ceram. Soc.* 96, 710–718. doi:10.1111/jace.12160

Chen, Y., Sun, J., Jiang, P., Chai, Z., Zhang, B., and Li, J. (2023). Review on porous ceramic-based form-stable phase change materials: preparation, enhance thermal conductivity, and application. *ChemBioEng Rev.* 10, 941–958. doi:10.1002/cben.202300023

Cologna, M., Francis, J. S. C., and Raj, R. (2011). Field assisted and flash sintering of alumina and its relationship to conductivity and MgO-doping. *J. Eur. Ceram. Soc.* 31, 2827–2837. doi:10.1016/j.jeurceramsoc.2011.07.004

He, X., Wang, M., Jin, T., and Li, L. (2024). Characterization and photocatalytic properties of porous ZrO_2/Al_2O_3 ceramic bead supported BiOI catalyst. *Ceram. Int.* 50, 12529–12538. doi:10.1016/j.ceramint.2024.01.162

Li, Y., Xu, C., Huang, R., Zhao, X., Wang, X., and Jia, Z. (2023). Mechanism analysis of arc-induced flash sintering of 3YSZ at room temperature. *J. Eur. Ceram. Soc.* 43, 7033–7040. doi:10.1016/j.jeurceramsoc.2023.07.019

Lin, H., Shen, Q., Ma, M., Ji, R., Huo, H., Qi, H., et al. (2025). 3D printing of porous ceramics for enhanced thermal insulation properties. *Adv. Sci.* 12, 2412554. doi:10.1002/advs.202412554

Liu, J., Li, X., Wang, X., Huang, R., and Jia, Z. (2020). Alternating current field flash sintering 99% relative density ZnO ceramics at room temperature. *Scr. Mater.* 176, 28–31. doi:10.1016/j.scriptamat.2019.09.026

Liu, Z., He, Z., Li, Z., Chen, S., Cheng, L., Zhao, X., et al. (2025). Large-diameter ceramic room-temperature flash sintering technology based on new carbon electrodes. *J. Adv. Ceram.* 14, 9221094. doi:10.26599/JAC.2025.9221094

Naik, K., Jha, S. K., and Raj, R. (2016). Correlations between conductivity, electroluminescence and flash sintering. *Scr. Mater.* 118, 1–4. doi:10.1016/j.scriptamat.2016.03.001

Nie, J., Zhang, Y., Chan, J. M., Huang, R., and Luo, J. (2018). Water-assisted flash sintering: flashing ZnO at room temperature to achieve ~98% density in seconds. *Scr. Mater.* 142, 79–82. doi:10.1016/j.scriptamat.2017.08.032

Roy, T. K. (2015). Assessing hardness and fracture toughness in sintered zinc oxide ceramics through indentation technique. *Mater. Sci. Eng. A Struct. Mater. Prop. Microstruct. Process.* 640, 267–274. doi:10.1016/j.msea.2015.05.107

Shahini, S., Judge, W. D., Tam, J., and Azimi, G. (2018). Design, fabrication, and characterization of porous yttria-stabilized zirconia ceramics for hot gas filtration applications. *Adv. Eng. Mater.* 20, 1700941. doi:10.1002/adem.201700941

Shakir, R. A., and Géber, R. (2023). Structure and properties of ZrO_2–Al_2O_3–MgO porous ceramic for biomedical applications. *Results Eng.* 18, 101104. doi:10.1016/j.rineng.2023.101104

Wang, Q., Zhao, X., Xiao, Y., Li, Y., Kang, S., Guo, J., et al. (2025). Cold sintering of large-sized ZnO varistor ceramics: unlocking superior non-ohmic behavior and breakdown strength via targeted thermal treatment. *Rare Met.* 44, 8979–8994. doi:10.1007/s12598-025-03394-9

Zhao, X., Zhang, H., Wang, J., Zhao, X., Huang, R., and Wang, X. (2024). Flash sintering of silicon carbide at room temperature. *Ceram. Int.* 50, 35836–35841. doi:10.1016/j.ceramint.2024.06.323